Organic & Biomolecular Chemistry

Accepted Manuscript

ROYAL SOCIETY OF CHEMISTRY

www.rsc.org/obc

Journal Name

Dynamic Article Links ►

Cite this: DOI: 10.1039/c0xx00000x

www.rsc.org/xxxxxx

ARTICLE TYPE

Ionic Liquids as Porogens for Molecularly Imprinted Polymers: Propranolol, a Model Study

Katherine Booker,[a] Clovia I Holdsworth,[a] Cara M Doherty,[b] Anita J Hill,[b] Michael C Bowyer [c] and Adam McCluskey[a*]

Received (in XXX, XXX) Xth XXXXXXXXX 20XX, Accepted Xth XXXXXXXXX 20XX
DOI: 10.1039/b000000x

Abstract: The selectivity and rebinding capacity of molecularly imprinted polymers selective for propranolol (**1**) using the room temperature ionic liquids [BMIM][BF_4], [BMIM][PF_6], [HMIM][PF_6] and [OMIM][PF_6] and $CHCl_3$ were examined. MIP_{BF4}, MIP_{PF6} and MIP_{CHCl3} returned IF (imprinting factor) values of 1.0, 1.98 and 4.64 respectively. The longer chain HMIM and OMIM systems returned lower IF values of 1.1 and 2.3 respectively. MIP_{PF6} also displayed a ~25% binding capacity reduction vs. MIP_{CHCl3} (5 μ.mol/g vs. 7 μmol/g respectively). MIP_{CHCl3} and MIP_{PF6} differed in terms of BET surface area (306 m^2/g vs. 185 m^2/g), pore size (1.098 and 2.185 nm vs. 0.972 and 7.064 nm) and relative number of pores (Type A: 10.366 vs. 7.465%; Type B: 8.452 vs. 2.952%), and surface zeta potential (-37.9 mV vs. -20.3 mV). MIP specificity for **1** was examined by selective rebinding studies with caffeine (**2**) and ephedrine (**3**). Only low levels of **2**-binding, with more **2** rebound by MIP_{PF6} than MIP_{CHCl3}, but this was non-selective binding. Both MIP_{CHCl3} and MIP_{PF6} displayed a higher affinity for **3** than for **2**. Reduction in the Room Temperature Ionic Liquid (RTIL) porogen volume had little impact on polymer morphology, but did result in a modest decrease in IF from 2.6 to 2.3 and in binding capacity (30% to 19%). MIP_{CHCl3} retained highest template specificity on rebinding from $CHCl_3$ (IF = 4.6) dropping to IF = 0.6 on addition of [BMIM][PF_6]. MIP_{CHCl3} binding capacity remained constant using $CHCl_3$, CH_2Cl_2 and MeOH (46-52%), dropped to 6% on addition of [BMIM][PF_6] and increase to 83% in H_2O (but at the expense of specificity with IF_{H2O} = 1.4). MIP_{PF6} rebinding from MeOH saw an increase in specific rebinding to IF = 4.9 and also an increase in binding capacity to 48% when rebinding **1** from MeOH and to 42% and 45% with H_2O and CH_2Cl_2 respectively, although in the latter case increased capacity was at the cost of specificity with IF_{CH2Cl2} = 1.2. Overall MIP_{PF6} capacity and specificity were enhanced on addition of MeOH.

Introduction

Molecularly imprinted polymers (MIPs) are a specialty class of polymers that possess a cavity specific to their original template. MIPs synthesis requires four basic ingredients: a template (T); a functional monomer (FM); a crosslinking agent to impart stability and cavity rigidity; and a porogen in which to conduct the polymer synthesis.[1-4]

With thousands to millions of highly specific template binding pockets, MIPs possess the ability to recognize and (re)bind specific target molecules.[5] Whilst they are the chemical counterparts to biological receptors, they are robust, insoluble in most media and in most cases lack the natural homogeneity of active sites associated with biological receptors. The population of binding sites in MIPs is typically heterogeneous because of the influence of the equilibria that govern the monomer–template complex formation and the dynamic of the growing polymer chains prior to copolymerization. The nature and distribution of binding sites are influenced by the method of MIP synthesis (see below) of which there are ostensibly two approaches; covalent and non-covalent. With the former, post polymerization template removal requires destruction of the covalent linker generating a cavity (binding site) that complements the size, shape and electronic properties of the template.[6] With the non-covalent, self-assembly, approach the template, functional monomer and cross-linking agents are equilibrated to generate a pre-polymerisation cluster utilizing hydrogen bond interactions, electrostatic attraction and associated weak interactions.[7] The mix is then polymerized to generate cavities on subsequent removal of the template via exhaustive extraction.[8]

MIP technology has been applied across a myriad of areas including, but not limited to, separation and isolation, antibody and receptor mimics, and biosensor style devices. Their shelf stability, robustness and reusability mean that they are highly usable and flexible. The variety of molecules 'imprinted' is impressive in both breadth of template and also diversity highlighting the utility of MIPs. The general MIP area has been extensively reviewed over the past decade.[9-13] More recently efforts have focused on garnering a greater understanding of the role of the template on MIP morphology and function, as well as the role of the porogen in the initial MIP synthesis. In this latter regard we are one of the few groups who have explored the potential use of room temperature ionic liquids as porogen.[14,15]

The tunable nature of an ionic liquids' solvating properties holds considerable potential to facilitate an increase in favourable

FM–T interactions,[16,17] whilst potentially eradicating those associated with non-specific binding.[1,9,18] An additional attraction of RTILs as porogens is the considerable body of literature pertaining to polymerization rate enhancements (which allows precipitation polymerization approaches to be applied in a short time frame),[19,20] and our earlier studies that showed an enhancement of MIP selectivity relative to the same MIPs manufactured in a traditional volatile organic compound (VOC) porogen.[14,15] Herein we report our recent efforts using propranolol (**1**) as a model template.

Results and Discussion

Propranolol (**1**) is one of the most widely studied templates in the MIP field, with multiple high specificity systems reported (Figure 1).[21-28] This makes **1** an ideal model template to explore the effect of RTILs as porogens. In traditional MIP studies, porogens are selected that will promote template-monomer interactions, typically apolar volatile organic compounds.[29] However, RTILs consist of charged species and exhibit different intra-liquid structural properties.[30] This study focuses on [BMIM][BF_4], [BMIM][PF_6] and modifications to the cation's alkyl chain.

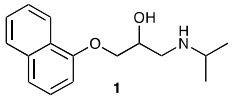

1

Figure 1. Chemical structure of racemic propranolol (**1**).

As with all of our imprinting studies, molecular modelling – NMR titrations (MM-NMR) were conducted to determine the most appropriate FM:T ratios, but also in this instance to explore, and subsequently minimize (thorough experimental design) any unfavourable interactions between the selected RTILs and **1**.[14,15] These modelling evaluations examined the potential interactions between ethylene glycol dimethyl acrylate (EGDMA) and divinyl benzene (DVB) as cross linkers. Here we noted that there were strong, and thus unfavourable interactions with EGDMA, but no such interactions with DVB. All MM-NMR examinations indicated favourable interactions between **1** and the FM, methacrylic acid (MAA), with maximal interaction at a 1:4 ratio in keeping with previous reports.[29] Both [BMIM][BF_4] and [BMIM][PF_6] showed strong hydrogen bonding interactions with **1** through the F-atoms to the NH of **1**.[31] [BMIM][BF_4] displayed a stronger H-bonding interaction (2.2 Å) than [BMIM][PF_6] (1.8 Å) (ESI†). In addition we also developed a conventional MIP using MAA to allow determination of the effect of the RTIL on MIP specificity and capacity. Molecular modelling evaluations clearly showed excellent levels of interaction between **1** and MAA with the most favourable interactions noted at a 4:1 (FM : T) ratio (ESI†). Both [BMIM][BF_4] and [BMIM][PF_6] also showed clear evidence of interaction with MAA. This was of some concern as in an ideal scenario only interactions between the FM and T would be present. We found no such unfavourable interactions with any of the other pre-polymerisation cluster components, e.g. the cross linker divinylbenzene (DVB) (data not shown). With this in mind we also evaluated the more complex system in which all MIP recipe components were present, and noted favourable interactions between the FM and T, but the unfavourable interactions between [BMIM][PF_6] and the FM, and [BMIM][PF_6] and **1** were retained. Thus the combination of MAA and DVB was deemed to be the most suitable for the development of subsequent MIPs. This combination of cross linker and functional monomer has been used previously in the development of selective MIPs.[31-35]

MIPs were subsequently synthesised using [BMIM][BF_4] (MIP_{BF4}), [BMIM][PF_6] (MIP_{PF6}) and $CHCl_3$ (MIP_{CHCl3}) as the porogens. As we have previously noted, the use of RTILs resulted in higher polymer yields and shorter polymerisation times (see experimental).[14,15] Selective imprinting was defined as, IF (Imprinting Factor) = [concentration of template rebound by MIP] / [concentration template rebound by NIP (non-imprinted polymer) ‡]. Rebinding of **1** reached equilibrium at 6 h (ESI†, Fig. S3A-D). MIP_{BF4}, MIP_{PF6} and MIP_{CHCl3} returned IF values of 1.0, 1.98 and 4.64 respectively under the conditions used herein. The IF value obtained with MIP_{CHCl3} was in keeping with previous literature reports.[21-28] The MIP_{PF6} reduced specificity (relative to MIP_{CHCl3}), as presumably was the lack of an imprinting effect with MIP_{BF4} was a function of the reduced level of FM-T interaction predicted by the MM-NMR approach and a consequence of the ion pair nature of the RTILs examined. MIP_{PF6} also displayed a ~25% binding capacity reduction vs. MIP_{CHCl3} (5 µmol/g vs. 7 µmol/g respectively; ESI†).

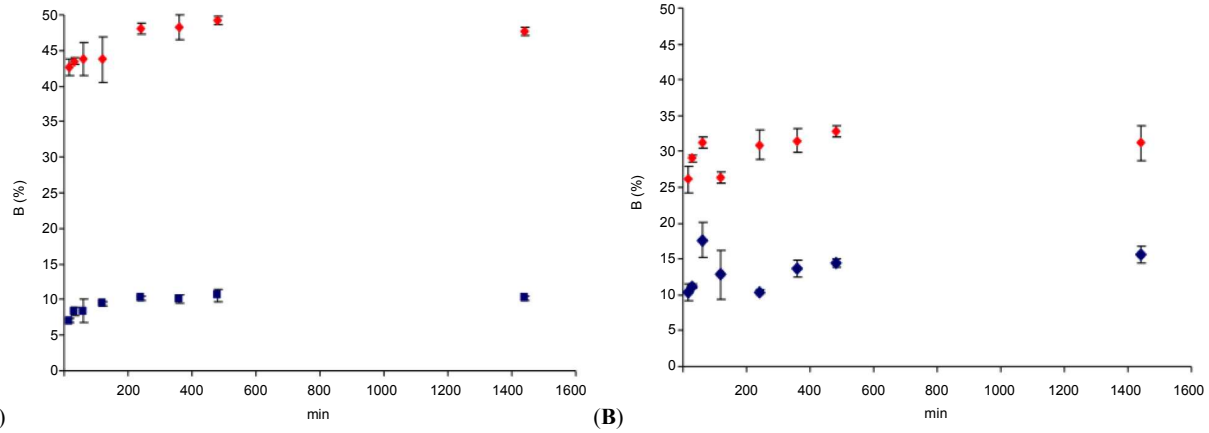

Figure 2. Rebinding from 5 mL of a 25 µM solution of **1** in $CHCl_3$ over 24hr time period using (**A**) ◆MIP_{CHCl3}, (■ NIP_{CHCl3}); and (**B**) ◆MIP_{PF6}, (◆NIP_{PF6})

As can be seen from Figure 2B, MIP_{PF6} and NIP_{PF6} showed an initial spike in rebinding (not seen in MIP_{CHCl3}; Figure 2A). We attribute this to larger surface pores evident in MIP_{PF6}, which resulted in fast rebinding kinetics, albeit at the expense of selectivity. As our focus here was to highlight the porogenic character differences between VOC and ionic liquids on the specific rebinding of the template we limited our evaluation to the Scatchard plot analysis of MIP_{CHCl3} and MIP_{PF6}.[36-38] It is known

that MIP synthesis in ionic liquids affects polymer formation in non-imprinted polymers and this impact is evident from Figure 2.[39-41] Our Scatchard analysis of the MIPs rebinding of **1** confirmed, and was consistent with previous finding, the homogeneous nature of the binding site distribution (Table 1) (ESI†).[42,43]

Table 1 The binding affinity (K_d), number of binding cavities (N_T) values obtained from Scatchard plots of the binding isotherms of MIP_{CHCl3} and MIP_{PF6}.

Porogen	K_d (M)	N_T (mole)	ΔG_{bind} [a] (kJ mol^{-1})
$CHCl_3$	3.34x 10^{-5}	1.37 x 10^{-5}	-25.54
[BMIM][PF_6]	1.60 x 10^{-5}	9.77 x 10^{-6}	-27.36

MIP_{CHCl3} has a K_d value more than twice that of MIP_{PF6} (1.37 x 10^{-5} vs. 9.77 x 10^{-6}) consistent with the observed differences in binding capacity and presumably with less well-defined cavities (Table 1). The decrease in MIP_{PF6} binding capacity may have been a consequence rapid polymerisation kinetics, which limits the thermally driven template/functional monomer equilibrium processes necessary for the formation of MIP binding cavities.[44]

Polymer morphology

Whilst both preparations show template selectivity, MIP_{CHCl3} preparation clearly has higher imprinting selectivity (IF = 4.64) for the template than MIP_{PF6} (IF = 1.98 at t = 6h). Examination of the physicochemical properties of MIP_{CHCl3} and MIP_{PF6} highlighted differences in the BET surface area, PALS pore size and relative number of pores, and surface zeta potential (Table 2).

Table 2. Selected physicochemical properties of propranolol NIP / MIP_{CHCl_3} and propranolol NIP / $MIP_{[bmim]PF6}$.

Polymer system	BET Specific surface area (m^2/g)	BET Pore volume (cm^3/g)	PALS Diameter of Type A pores (small) (nm)	Relative Number of Type A Pores (%)	PALS Diameter of Type B pores (large) (nm)	Relative Number of Type B Pores (%)	Zeta Potential (mV)
MIP_{CHCl_3}	306	0.201	1.098	10.336	2.185	8.452	-37.9
NIP_{CHCl_3}	509	0.282	1.143	10.618	2.229	12.691	-36.6
$MIP_{[bmim]PF_6}$	185	0.295	0.972	7.465	7.064	2.952	-20.3
$NIP_{[bmim]PF_6}$	180	0.302	0.921	5.155	11.145	2.838	-17.0

The major NIP_{CHCl3} vs. MIP_{CHCl3} difference was found in the BET surface area with the NIP_{CHCl3} displaying 1.6 times the surface area of MIP_{CHCl3}. This suggested that the template influenced polymer morphology,[45] but only in the case of the VOC systems, the corresponding [BMIM][PF_6] systems have essentially identical surface areas at 180 and 185 m^2/g for NIP and MIP respectively. Determination of MIP specificity is traditionally measured as the imprinting factor (the ratio of binding of the MIP vs. the NIP). An inherent assumption in this determination is that excepting the template, all other factors are identical and consequently the comparison is that of like-vs-like. However it is known that the template effects the interaction of all pre-polymerisation components, and in turn this can impact the physical properties of the resultant polymers.[45] In this instance the template interaction results in a significantly lower surface area.[46,47] Notwithstanding this it is clear that imprinting has occurred evidenced both by the change in polymer characteristics and the specific reminding of the template observed. The pore size and relative number of pores of MIP_{CHCl3} and MIP_{PF6} (and NIP_{CHCl3} and MIP_{PF6}) were determined by Positron Annihilation Lifetime Spectroscopy (PALS).[48] In both instances, the PALS data shows the presence of two distinct pore types present in both MIP and NIP (Table 2). These pores are categorised as small and large (type A and type B respectively). MIP_{CHCl3} and NIP_{CHCl3} display consistent pore sizes at 1.1 (type A) and 2.2 nm (type B) respectively, only differing in the number of type B pores with the NIP_{CHCl3} having a greater relative number (12.961 vs 8.452%). The PF_6 systems displayed lower numbers and smaller type A pores (0.921 and 0.972 nm, MIP vs. NIP respectively), and lower numbers of, but significantly larger type B pores (11.145 and 7.064 nm, MIP vs. NIP respectively) than the equivalent $CHCl_3$ systems. Type A pores of MIP_{PF6} and NIP_{PF6} are of the same dimensions, but are more frequent in MIP_{PF6} (7.465 vs. NIP_{PF6} at 5.155). The NIP_{PF6} type B pores (11.145 nm diameter) are 1.6 times larger than the MIP_{PF6} type B pores (7.064 nm diameter) with a comparable number in both the MIP_{PF6} and NIP_{PF6}. It is tempting to relate the difference in type A pore numbers to specific cavity formation in MIP_{PF6}. However, at its widest points, the imidazolium moiety measures 0.967 x 0.3071 nm; PF_6 measures 0.328 x 0.328 nm and **1** measures 1.3596 x 0.7962 nm. Thus **1** cannot be accommodated by the type A pores (diameter ranging from 0.914 - 1.141 nm) and is thus unlikely to have been involved in the formation of these cavities in either of the polymer preparations. The type B pores are all capable of accommodating **1**, even in the MIP_{CHCl3} polymer preparation where the type B pores are significantly smaller than those in the [BMIM][PF_6]-prepared polymer. It is therefore a reasonable assumption that the specific binding taking place occurs in these type B pores, and the significantly larger number (2.8 times) of these present in MIP_{CHCl3} polymer preparation is responsible for the higher levels of template uptake in these polymers. Rosengren *et al* reported that the pore size distribution could be modified as a function of FM:CL ratio. In their studies with warfarin 3-4 nm pore distribution was deemed optimal.[49] In this study the FM:CL is fixed and it is most probable that the variations in pore size reflect the interaction of the template with local IL domains with H-bonding generating a template-IL hybrid that subsequently generates a large pore. We attribute the increase in specific binding capacity in MIP_{CHCl3} to a higher frequency of type B pores capable of accommodating a molecule of **1**. The decrease in MIP_{PF6} selectivity may be a consequence of non-specific template binding in type B pores.

The PALS data correlate well to another study involving the preparation of cross linked polymers in VOCs compared to RTILs, which also showed larger pore sizes and decreased surface areas in RTIL-prepared polymer when using toluene and 1-octyl-3methylimidazolium bis((trifluoromethyl)sulfonyl)imide as VOC and RTIL, respectively.[50] It was hypothesised that the large pore volumes observed in polymers prepared with RTILs as porogens arises from the more structured arrangement of RTIL molecules compared to VOCs[51] which may result in the RTIL forming a 'micellar' structure (as proposed by Triolo *et al*.[30]). The relatively larger size of these 'micelles' compared to VOC molecules permeating the polymer structure would explain the discrepancy in pore size.

Another feature that impacts on rebinding is the polymer

surface Zeta potential. The data presented in Table 2 shows the difference in surface charge between the $CHCl_3$ and PF_6 systems. MIP_{CHCl3} returned a Zeta potential of 37.9 mV vs. MIP_{PF6} 20.3 mV, and these values reflect the observed differences in the polymer particles by TEM. MIP_{CHCl3} showed higher particle dispersion in solution than MIP_{PF6}. The MIP_{PF6} lower surface charge was most likely an indication of a reduction in the number of surface MAA, with a concomitant reduction in surface binding taking place.

Scanning electron microscopy (SEM) and tunnelling electron microscopy (TEM) were used to examine the gross morphologies of the polymers produced in $CHCl_3$ and [BMIM][PF_6]. The SEM image of MIP_{CHCl3} shows discrete spherical particles of 1-3 μM in diameter (Figure 3A). The SEM image of NIP_{CHCl3} also showed the presence of discrete spherical particles, but with a wider range in particle size (Figure 3B).[14,15] Neither MIP_{PF6} nor NIP_{PF6} SEM images showed evidence of discrete particles, but rather an aggregation of 300-500 nm sized particles.

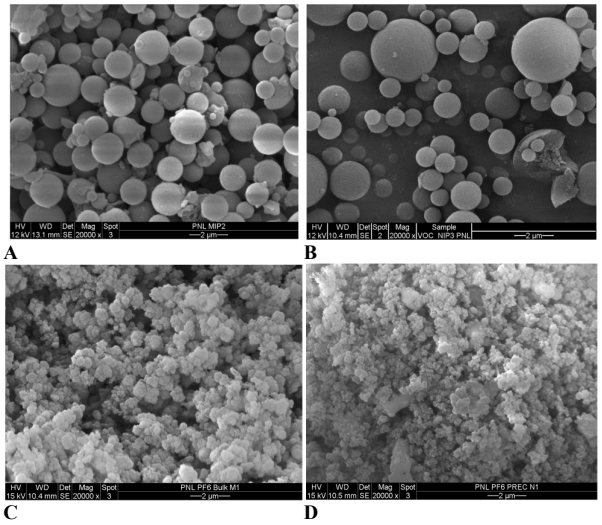

Figure 3. SEM images of **1**-imprinted polymers (**A**) MIP_{CHCl3}, (**B**) NIP_{CHCL3}, **(c)** MIP_{PF6}; and **(d)** NIP_{PF6}.

Using CH_3CN as the dispersion solvent, TEM analysis of MIP_{CHCl3} confirmed the SEM findings (Figure 4A). MIP_{PF6} under TEM analysis revealed the retention of aggregated clusters of a very fine particulate nature.

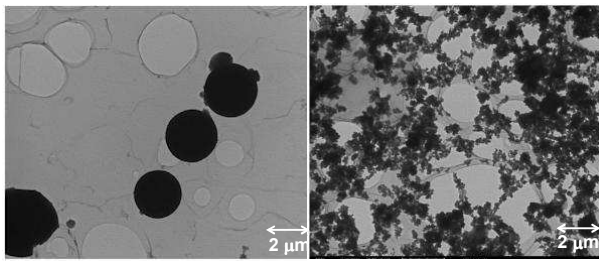

Figure 4. TEM images of **1**-imprinted polymers (**A**) MIP_{CHCl3}; and (**B**) MIP_{PF6}.

TGA showed similar decomposition processes in MIP_{CHCl3} and MIP_{PF6} with the onset of decomposition at 300 °C and second decomposition phase at ~ 375 ºC. MIP_{CHCl3} was marginally more stable than MIP_{PF6} (ESI†).

As we previously noted with cocaine-imprinted systems, the RTIL-prepared polymer exhibit significantly less swelling than the VOC-prepared polymers.[14,15] However, in both cases, the MIP showed a higher degree of swelling than the NIP (MIP_{CHCl3} = 120%; NIP_{CHCl3} = 83%; MIP_{PF6} = 34%; NIP_{PF6} = 11%). This may indicate the presence of rebinding cavities in the MIPs. These results were a good indication that the RTIL-prepared polymer would maintain a higher degree of binding site integrity in solution than the VOC polymer preparations.

*Cross reactivity with caffeine (**2**) and ephedrine (**3**)*

In order to assess the **1**-MIP specificity we examined both MIP_{CHCl3} and MIP_{PF6} for their ability to selectively rebind caffeine (**2**) and ephedrine (**3**) (Figure 5). These data are presented in Table 3.

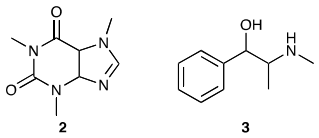

2 **3**

Figure 5. Chemical structures of caffeine (**2**) and ephedrine (**3**).

Table 3. Imprinting factor and rebinding capacity of MIP_{CHCl3} and MIP_{PF6} for **1** and specificity and cross reactivity data for **2** and **3**. Studies were conducted at 6 h rebinding times using 25 μM $CHCl_3$ solutions of each analyte.

MIP	Target	IF	Binding capacity (%)
MIP_{CHCl3}	**1**	4.8	48
	2	0.3	2.6
	3	3.6	37
MIP_{PF6}	**1**	2.6	31
	2	0.8	9.6
	3	1.5	33

As anticipated there was only low levels of binding of **2** with both MIP systems for both polymers. Rebinding of **2** was higher with MIP_{PF6} than MIP_{CHCl3}, but neither exhibited selectivity with IF values of 0.8 and 0.3 respectively (Table 3). This reflected the significant structural differences between **1** and **2**. The low binding of **2** was attributed to the difference in three dimensional and electronic structures of **2**. Both MIP_{CHCl3} and MIP_{PF6} displayed a higher affinity for **3** than for **2**, reflecting the structural and electronic similarity of **3** and **1**.

MIP_{CHCl3} rebound a higher quantity of **1** than **3** (48% compared to 37%) with NIP_{CHCl3} binding remaining constant (10%), resulting in a reduction in IF value from IF = 4.8 for **1** and IF = 3.6 for **3**. A reduction in IF MIP_{PF6} was also evident from IF = 2.6 for **1** to IF = 1.5 for **3**. The lack of MIP_{PF6} discrimination of 1 over 3 did not correlate with the K_d values extracted from the Scatchard analysis (Table 1). The MIP_{PF6} K_d value of 1.60 x 10^{-5} (vs. 3.34 x 10^{-5} for MIP_{CHCl3}) indicated more well-defined binding cavities in MIP_{PF6} than in MIP_{CHCl3}. However, the quantity of **3** bound for both MIPs was comparable and suggests that the relatively fewer number of binding sites in MIP_{PF6} and the corresponding lower rebinding capacity may be responsible for the lower levels of selectivity in MIP_{PF6}. Or that the smaller **3** positions the key moieties in the correct chemical space to maximise retention within the binding sites. This would effectively mask any differences in selectivity for **1** over **3** in MIP_{PF6}. Other studies have also reported high levels of binding for structurally analogous compounds with **1**-imprinted polymers, where binding levels for analytes such as pindolol and acebutolol are actually higher than for **1** itself.[52] Discrimination of the MIP for **1** may also be limited slightly by the use of a mixture of enantiomers as template, which would increase the heterogeneity of binding sites and reduce the ability of the polymer to distinguish between structurally analogous compounds.

Factors Affecting Rebinding Performance - Polymerisation Solvent Volume

We have previously demonstrated with cocaine selective MIPs that the polymerisation volume affects the MIP rebinding performance.[14,15] Reduction in RTIL porogen volume from 30 to 5 mL was examined, but little impact on polymer morphology by SEM analysis was noted (Figure 6).

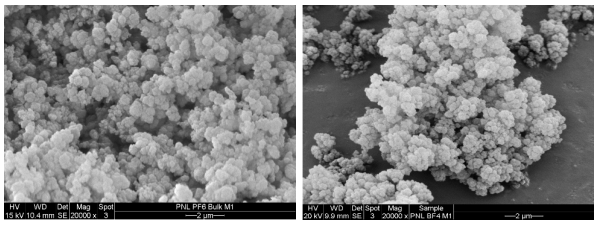

A **B**

Figure 6. SEM images of MIP_{PF6} synthesised in (**A**) 30 mL; and (**B**) 5mL $[BMIM][PF_6]$.

Subsequent rebinding analysis indicated a reduction in binding capacity with the $[BMIM][PF_6]$ 5 mL polymer to 19% compared with 30% with the $[BMIM][PF_6]$ 30mL preparation (30%), in turn lower than the 48% rebinding noted with MIP_{CHCl3} (Table 3). MIP_{PF6} (5 mL) returned an IF = 2.3 comparing favourably with MIP_{PF6} (30 mL) at IF = 2.6.

The reduced binding capacity of **1** with MIP_{PF6} (5 mL) was in keeping with prior reports indicating that a reduction in porogen volume leads to a reduction in polymer surface area and binding capacity reduction.[53,54] It was also possible that the enhanced binding capacity of MIP_{PF6} (30 mL) resulted from increased porogen permeation into the polymer system, or higher levels of polymer solubility (which would lead to a later phase separation and higher surface area).[29] However the high viscosity of $[BMIM][PF_6]$ favours the latter possibility.

Effect of Rebinding Solvent

MIP efficacy is generally examined using the original porogen for rebinding, here $CHCl_3$ and $[BMIM][PF_6]$. However in the $[BMIM][PF_6]$ viscosity proved to be a limiting factor. We investigated MIP_{CHCl3} and MIP_{PF6} rebinding in a range of alternative solvents (Table 4). $CHCl_3$ was replaced by methanol as this permits the evaluation of the addition of $[BMIM][PF_6]$ (not $CHCl_3$ miscible).

Table 4. MIP_{CHCl3} and MIP_{PF6} imprinting factors in MeOH and MeOH / $[BMIM][PF_6]$ mixed solvent systems.

Solvent System	MIP_{CHCl3} (IF)	Binding	MIP_{PF6} (IF)	Binding
$CHCl_3$	4.6	46%	-	-
$[BMIM][PF_6]$	-	-	2.0	26%
CH_3OH	2.3	47%	3.8	48%
80% CH_3OH / 20% $[BMIM][PF_6]$	0.6	6%	4.9	14%
H_2O	1.4	83%	2.2	42%
CH_2Cl_2	1.2	52%	1.2	45%

Table 4 shows the outcome of rebinding studies in the listed rebinding solvents. MIP_{CHCl3} shows the highest specificity when rebinding was conducted in the original porogen (IF = 4.6) dropping to an IF = 0.6 on addition of $[BMIM][PF_6]$. The binding capacity of MIP_{CHCl3} remains constant using $CHCl_3$, CH_2Cl_2 and MeOH (46-52%), but drops to 6% on addition of $[BMIM][PF_6]$ and increase to 83% in H_2O (but at the expense of specificity with IF_{H2O} = 1.4). MIP_{PF6} with the exception of CH_2Cl_2 (IF = 1.2) saw an increase in specific rebinding, with the highest IF of 4.9 noted from MeOH. MIP_{PF6} saw a substantial increase in binding capacity (to 48%) when rebinding **1** from MeOH and also to 42% and 45% with H_2O and CH_2Cl_2 respectively, although in the latter case increased capacity was at the cost of specificity with IF_{CH2Cl2} = 1.2.

With MIP_{PF6} both capacity and specificity were enhanced on addition of MeOH. Other reports of rebinding of **1** have suggested that non-polar solvents promote rebinding based on H-bonding of the template to the functional monomer whereas in polar environments there may be hydrophobic processes, such as π- π stacking interactions of the naphthalene rings of the template with the aromatic ring on the crosslinker, DVB.[52,55] We have used such solvophobic effects to good effect with poorly functionalised aromatic templates previously, and are in keeping with the observed increases in rebinding capacity on increasing the solvophobic effect as evidenced with both MeOH and H_2O as the rebinding solvents.[56-58] The increased binding capacity noted was consistent with methanol acting as a better polymer dispersant, increasing **1**'s access to binding sites, hence increasing **1**-rebinding. The use of MeOH has previously been shown to decrease unfavorable self-association of the template reducing non-specific interactions, and this may have played a role in the increased specific binding noted with **1** and **2** using MeOH as the porogen, it is possible that a similar effect results from the use of $[BMIM][PF_6]$ as porogen.[59,60]

Influence of alkyl chain length on RTIL porogen and the imprinting of 1

Although the imprinting of **1** has been successfully achieved using $[BMIM][PF_6]$ as polymerisation solvent, this work has been shown that not all RTILs will have a similar effect.

One very significant difference between RTILs and conventional solvents is the heterogeneous behaviour displayed by many RTILs in the liquid state. This effect has been shown to increase as a function of the alkyl chain length of the side chain in imidazolium-based RTILs.[30] The butyl side chain has been reported in a number of studies to be the transitional point between a homogenous composition of the RTIL and one displaying long range order (with the degree of order increasing with the side chain length). As such, the ideal situation would then be to investigate imidazolium-based RTILs with ethyl, butyl and hexyl side chains. However, solubility of the polymer components, particularly the crosslinker DVB becomes a significant factor with the ethyl side chain RTILs. Therefore, instead of investigating the difference between the heterogeneous and homogenous RTILs, this study will instead simply investigate the effect of the increase in long range order. RTILs with butyl, hexyl and octyl imidazolium side chains were selected for analysis.

A major issue with increasing alkyl chain length was an increase in viscosity from 450 cP (butyl) to 682 cP (octyl).[61] This increased viscosity adversely impacts on mass transport for any rebinding study. This is also evidenced in the SEM images of the resultant MIPs, which show a greater degree of particle agglomeration (Figure 7).

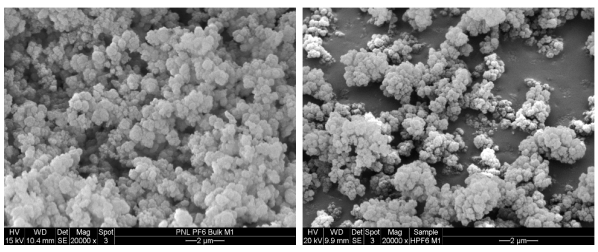

A B

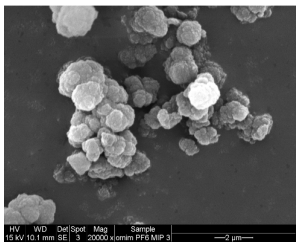

C

Figure 7. SEMs of MIPs prepared in **(a)** [BMIM][PF_6], **(b)** [HMIM][PF_6] and **(c)** [OMIM][PF_6].

There was little difference between the swelling of the [BMIM] and [HMIM] based systems at 34% and 33% respectively. However the [OMIM][PF_6]-prepared MIP showed only 6% swelling. Similarly, by TGA examination the [BMIM], [HMIM] and [OMIM] produced polymers showed a similar onset of decomposition at approximately 270 °C and two decomposition phases. The thermal stability of the polymers increases with increasing alkyl chain length through the initial decomposition phase. There are slight differences in the secondary stage of decomposition, with thermal stability increasing in the order of [HMIM] ≈ [OMIM] > [BMIM] (ESI†).

Rebinding studies revealed no imprinting with the HMIM based MIP (IF = 1.1) but modest levels of imprinting with the OMIM system (IF = 2.1). The major physical changes in the MIP generated with variations in the imidazolium cation alky substituent were related to viscosity and the increasing structure of the ionic liquid. These physical property changes impact on the imprinting of **1**.

The lower levels of binding in the [HMIM][PF_6] and [OMIM][PF_6] polymer preparations could be a function of the high viscosity of the RTIL. However, while the [HMIM][PF_6] polymer preparation shows very little selectivity for the template, the [OMIM][PF_6]-prepared polymer does, with an IF = 2.1. This suggests that there is something in the nature of the [OMIM][PF_6] which allows for the creation of additional imprinted cavities. This may well be related to the long range order present in the RTIL and the presence of nano-domains within the RTIL structure which may afford a pseudo surface imprinting effect. This may counteract some of the negative impact of solvent viscosity, where the template may have difficulty in moving through the RTIL.[62] If large domains are present in the solvent where the template can form associations with the monomer without needing to travel through the bulk of the solvent, there may be potential for the creation of a greater number of imprinted cavities which are template-selective within the polymer structure.

Conclusion

Rebinding of **1** reached equilibrium at 6 h and MIP_{BF4}, MIP_{PF6} and MIP_{CHCl3} returned IF values of 1.0, 1.98 and 4.64 respectively. MIP_{PF6} also displayed a ~25% binding capacity reduction vs. MIP_{CHCl3} (5 μmol/g vs. 7 μmol/g respectively). MIP_{CHCl3} rebinds **1** with a lower affinity than MIP_{PF6} (K_d values of 3.34 x 10^{-5} and 1.60 x 10^{-5} respectively), but this lack of affinity was compensated for by enhanced numbers of binding cavities with 1.37 x 10^{-5} vs. 9.77 x 10^{-6} for MIP_{PF6}.

The gross physicochemical properties of MIP_{CHCl3} and MIP_{PF6} differed in terms of BET surface area (306 m^2/g vs. 185 m^2/g), pore size (1.098 and 2.185 nm vs. 0.972 and 7.064 nm) and relative number of pores (Type A: 10.366 vs. 7.465%; Type B: 8.452 vs. 2.952%), and surface zeta potential (-37.9 mV vs. -20.3 mV). The RTIL-prepared polymer exhibited lower levels of swelling than the VOC-prepared systems. The MIP showed a higher degree of swelling than the NIP (MIP_{CHCl3} = 120%; NIP_{CHCl3} = 83%; MIP_{PF6} = 34%; NIP_{PF6} = 11%).

MIP specificity for **1** was examined by selective rebinding studies with caffeine (**2**) and ephedrine (**3**). Only low levels of **2**-binding, with more **2** rebound by MIP_{PF6} than MIP_{CHCl3}, but this was non-selective binding. Both MIP_{CHCl3} and MIP_{PF6} displayed a higher affinity for **3** than for **2**, reflecting the structural and electronic similarity of **3** and **1**.

Reduction in RTIL porogen volume from 30 to 5 mL was examined, but little impact on polymer morphology by SEM analysis was noted, but did result in a modest decrease in IF from 2.6 to 2.3 on reduction of porogen volume to 5 mL. More striking was a reduction in binding capacity to 19% (from 30%) Increasing RTIL viscosity had an adverse effect on observed IF with the HMIM based MIP IF = 1.1 and the OMIM system IF = 2.1.

Given the viscosity effects noted, we examined different rebinding solvents including binary systems. MIP_{CHCl3} retained its highest specificity when rebinding was conducted in the original porogen (IF = 4.6) dropping to an IF = 0.6 on addition of [BMIM][PF_6]. The binding capacity of MIP_{CHCl3} remained constant using $CHCl_3$, CH_2Cl_2 and MeOH (46-52%), but dropped to 6% on addition of [BMIM][PF_6] and increase to 83% in H_2O (but at the expense of specificity with IF_{H2O} = 1.4). MIP_{PF6} with the exception of CH_2Cl_2 (IF = 1.2) saw an increase in specific rebinding, with the highest IF of 4.9 noted from MeOH. MIP_{PF6} saw a substantial increase in binding capacity (to 48%) when rebinding **1** from MeOH and also to 42% and 45% with H_2O and CH_2Cl_2 respectively, although in the latter case increased capacity was at the cost of specificity with IF_{CH2Cl2} = 1.2. With MIP_{PF6} both capacity and specificity were enhanced on addition of MeOH.

Experimental

General Experimental

All solvents used were of bulk grade and redistilled. Propranolol hydrochloride was converted to the free base by treatment with NaOH to afford **1**, caffeine (**2**) and ephedrine (**3**) were purchased from Sigma-Aldrich and used as received. Methacrylic acid (MAA) and divinylbenzene were purchased from Sigma-Aldrich (Australia) and distilled under reduced pressure prior to use. Azobisisobutyronitrile (AIBN) was recrystallised from acetone and dried under vacuum prior to use. Chlorobutane, bromohexane, bromoethane and bromooctane (Sigma-Aldrich) were purified by washing with conc. H_2SO_4 until washings were colourless, neutralised with $NaHCO_3$ and dried with $MgSO_4$. The RTILs were synthesised in-house.

Molecular Modelling

Template-monomer molecular interactions were modelled using Spartan '04 software using the AM1 force field.[63,64] This molecular orbital computational method predicts the stable configuration of the template (T), functional monomer (FM), FM-FM clusters and T-FM clusters and calculates their standard heats of formation (ΔH_f). The molecules were randomly positioned and the T-FM clusters were modelled with respect to increasing the template-monomer ratio from 1 to 4. To account for the FM-FM interaction, the FM-FM clusters of up to five molecules were also surveyed. The energy of interaction of the T-M clusters, $\Delta E°_{(cluster)}$, at different molecular ratios were then calculated using the equation: $\Delta E_{interaction} = \Delta H_{f\ FM\text{-}T\ complex} - [\Delta H_{f\ monomer\ cluster} - \Delta H_{f\ template}]$.[65]

^{1}H NMR titration

Typically, from a stock solution of 500.0 mM in DMSO, incremental amounts of 50.0 μL of the functional monomer (MAA) was added to a 0.50 mL of 50.00 mM solution of **1** in deuterated DMSO. The proton signals from **1** were monitored as incremental amounts of monomers were added. The titration curve was then constructed from the plot of change in chemical shift, δ (ppm), of **1** against increasing amount of monomers added. All ^{1}H and ^{13}C NMR measurements were made using NMR Brüker 300 and 75 MHz respectively.

Polymer Synthesis

In a typical synthesis, molecularly imprinted polymers were prepared as follows. Pre-determined quantities of the template **1** (1.50 mmol, 389 mg), MAA (6.00 mmol, 509 µL), DVB (28.8 mmol, 4.103 mL) and AIBN (1 mmol %, 35.3 mg) were dissolved in the selected solvent (30 mL or 5 mL) in a reaction vial, purged with nitrogen gas for 5 min, sealed and polymerised at 60 ± 1.0 °C in a Thermoline oven for overnight. The polymers were then ground and sieved to a particle size <38 µm. The template was extracted via Soxhlet extraction with CH_3CN, toluene, methanol/acetic acid 70/30 v/v, methanol, CH_3CN, toluene, CH_3CN and methanol for 24 h before being dried under vacuum. The polymers were then dried at 40°C in a vacuum oven. A similar procedure was applied to non-imprinted polymers with the exception that no template was added.[66]

Time-Binding Study

Thirty milligrams, the optimal weight obtained from the adsorption study, was used for determining the optimum time of template binding. To a set of triplicate of 30.0 mg of polymer, 1.00 mL of 0.0800 mM **1** was added and the mixture shaken for a designated time of contact. The binding times investigated were 0.5, 2.0, 4.0, 7.0 and 18 hours. After binding, the mixtures were filtered and the filtrates analysed by HPLC. The amount of bound **1** was then obtained by subtracting the amount of **1** left in solution from the initial concentration. A plot of the amount of **1** bound versus time of contact was generated to determine the optimum time of contact for binding **1**.

Saturation Binding

The optimum weight and time of contact obtained from sorption and time-binding studies were used for the saturation binding experiments. A series of 20.0 mg of polymers were incubated with different concentrations of **1** for 6 h, after which, the mixtures were filtered and the filtrates analysed directly by HPLC. The amount of bound **1** was then obtained by subtracting the amount of **1** left in solution from the initial concentration. A plot of bound template against free **1** concentration was then generated to visualise the saturation binding isotherm of the polymers.

Scatchard analysis was performed as previously described.[67]

Binding measurements

Rebinding of **1** was measured using a Shimadzu Prominence HPLC equipped with SPD-20A/M20A lamp and LC-20AD pump. HPLC studies were conducted using a Shimadzu High Performance Liquid Chromatograph (LC-20AD) fitted with an econosphereTM C18, 5µm column (Grace®). For ephedrine analysis, the mobile phase consisted of 75% A (50mM phosphate buffer adjusted to pH3.5) and 25% B (3:7 water: acetonitrile, with 10mM TEA) (gradient elution). A 10µL injection volume was used with a run time of 10 min; flow rate of 0.8mL/min and detection wavelength of 190nm. Quantification was conducted using an external calibration method with a 7 point linear curve where R^2 = 0.995 at the concentration range of 10-1000µM. Results were analysed using Shimadzu LC Solution software. EPD concentration was monitored using the UV/VIS Photodiode Array Detector at a wavelength of 190nm. The mobile phase for caffeine consisted of a 70%/ 30% mixture of water/methanol. A 20µL injection volume was used with a run time of 5 min; flow rate 0.7mL/min and detection wavelength of 210nm. Quantification was conducted using an external calibration method with a linear curve of R^2 = 0.993 in the concentration range of 10- 100µM.

Scanning Electron Microscopy

Morphology of the polymers was examined using a Phillips XL30 scanning electron microscope. Each polymer was deposited on a sticky carbon tab and coated with gold using a SPI gold spotter coating unit. SEM micrographs of the polymers were obtained at 20000x magnification at 15.0 kV.

Swelling Measurements

Thirty milligrams of each polymer were packed into an NMR tube and the height of the dry polymer measured. A solution of **1** (1.00 mL of 0.0800 mM) in acetonitrile was added and allowed to soak for 24 h. Polymers were allowed to settle and the bed height of the swollen polymers was measured. The swelling factor was calculated from the ratio of the bed height of the swollen polymer to the dry polymer.

Zeta Potential

Zeta potential measurements were performed using a Malvern Nanosizer S fitted with a maintenance-free folded capillary cell (DTS 1060). Very dilute suspensions of polymers were prepared using ~ 0.75 mL deoxygenated distilled deionized water (non-equilibrated in air, 18.2 MΩ cm^{-1}). Measurements were performed at 25.0 °C, pH 7.0 in 5 replicates.

Specific Surface Area and Porosity (Brunauer-Emmett-Teller)

Nitrogen sorption analysis was carried out using a Micrometrics ASAP 2420 Accelerated Surface Area and Porosity instrument (Norcross, GA, USA). The analysis was carried out using 100 mg of sample and degassed at 110 ºC under vacuum for 16hr to remove any adsorbed solvent and water.. The specific surface area of each sample was determined from the adsorption data using the linearised BET equation.[68]

Positron Annihilation Lifetime Spectroscopy (PALS)

PALS measurements were performed using an automated EG&G instrument (Oak Ridge, TN, USA). The samples were analysed with a 30µCi ^{22}NaCl source sealed in a myler envelope. Analysis was performed under vacuum and 5 files of 4.5 x 10^6 integrated counts were measured for each sample. The spectra were deconvoluted using the LT Version 9 software and were fitted to 5 components. The first two components were related to the free and the *para*-positronium formation. The 3rd – 5th components were associated with *ortho*-positronium (*o*-Ps) formation which is related to the localisation of positronium within the pore space of the samples. The 3rd component's lifetime was fixed to 1.9 ns due to the free volume within the PMMA polymer chains. The 4th and the 5th components were related to the micro and mesopores within the templated samples. Each of the *o*-Ps component lifetimes were used to calculate the pore size and the corresponding intensities which are related to the relative number of pores within the samples. The pore size of the 4th component was calculated using the Tao-Eldrup model assuming infinitely long cylindrical pores.[69,70] Due to the longer lifetime, the pore size of the 5th component was calculated using the rectangular Tao–Eldrup (RTE) model based on an infinitely long channel.[71]

Acknowledgment

The authors acknowledge the financial support of the Australian Research Council and the Australian Federal Police Forensic Services. We also thank Professor Scott Donne for assistance with BET measurements.

References

1 K. Mosbach and O. Ramström, *Nature Biotech.*, 1996, **14**, 163.
2. G. Wulff and A. Sarhan, *Angew. Chem., Int. Ed. Engl.*, 1972, **11**, 341..
3. O. Bruggemann, K. Haupt, L. Ye, E. Yilmaz and K. Mosbach, *J. Chromatogr., A*, 2000, **889**, 15.
4. S. G. Bertolotti, C. M. Previtali, A. M. Rufs and M. V. Encinas, *Macromolecules*, 1999, **32**, 2920.
5. K. Haupt and K. Mosbach, Haupt, *Chem. Rev*. 2000, **100**, 2495.
6. R. J. Umpleby, S. C. Baxter, A. M. Rampey, G. T. Rushton, Y. Chen and K. D. Shimizu, *J. Chromatogr. B*, 2004, **804**, 141.
7. B. Tse Sum Bui and K Haupt, Anal Bioanal Chem. 2010, 398, 2481.
8. A. Ellwanger, S. Bayoudh, C. Crecenzi, L. Karlsson, P. K. Owens, K. Ensing, P. Cormack, D. Sherrington and B. Sellergren, *Analyst* 2001, **126**, 784.
9. A. McCluskey, C. I. Holdsworth and M. C. Bowyer, *Org. Biomol. Chem*., 2007, **5**, 3233.
10. K. Haupt, A. V. Linares, M. Bompart and B. T. Bui, *Topp. Curr. Chem.*, 2012, **325**, 1.
11. F. Puoci, G. Cirillo, M. Curcio, O. I. Parisi, F. Iemma and N. Picci, *Exp. Opin. Drug Deliv.*, 2011, **8**, 1379.
12. F. Puoci, F. Iemma and N. Picci, *Curr. Drug Deliv.*, 2008, **5**, 85.
13. Y. Fuchs, O. Soppera and K. Haupt, *Anal. Chim. Acta.*, 2012, **717**, 7.
14. K. Booker, M. C. Bowyer, C. J. Lennard, C. I. Holdsworth and A. McCluskey, *Aust. J. Chem.*, 2007, **60**, 51
15. K. Booker, M. C. Bowyer, C. I. Holdsworth and A. McCluskey, *Chem. Commun.*, 2006, 1730.
16. T. Welton, *Chem. Rev*., 1999, **99**, 2071.
17. J. P. Hallett and T. Welton, *Chem. Rev.*, 2011, **111**, 3508.
18. L. I. Andresson, *Analyst*, 2000, **125**, 1515.
19. Y. Vygodskii, E. Lozinskaya and A. Shaplov, *Polym. Sci. Ser. C.*, 2001, **43**, 2350;
20. M. Benton and C. Brazel, *Polym. Int*., 2004, **53**, 1113.
21. H. Kempe and M. Kempe, *Macromol. Rap. Commun.,* 2004, **25**, 315.
22. H. Kempe and M. Kempe, *Anal. Chem.,* 2006, **78**, 3659.
23. O. Castell, C. Allender and D. Barrow, *Biosens. Bioelect.* 2006, **22**, 526.
24. C. Hunt and R. Ansell, *Analyst* 2005, **131**, 678.
25. Y. Ma, G. Pan, Y. Zhang, X. Guo, H. Zhang, *J. Mol. Recognit*. 2013, **26**, 240.
26. S. Hajizadeh, C. Xu, H. Kirsebom, L. Ye, B. Mattiasson, *J. Chromatogr. A*. 2013,**1274**, 6.
27. O. Gurtova, L. Ye and F. Chmilenko. *Anal. Bioanal. Chem.,* 2013, **405**, 287.
28. L. N. Barde, M. M. Ghule, A. A. Roy, V. B. Mathur and U. D. Shivhare, *Drug Dev. Ind. Pharm*., 2013, **39**, 1247.
29. D. Spivak, *Adv. Drug Del. Rev.,* 2005, **57**, 1779.
30. A. Triolo, O. Russina, B. Fazio, R. Triolo and E. Di Cola, *Chem. Phy. Lett.,* 2008, **457**, 362.
31. Q. He, J. Yang, and X. Meng, *Chin. J. Chem. Phys.,* 2009, **22**, 517.
32. K. Yoshimatsu, K. Reimhult, A. Krozer, K. Mosbach, K. Sode, and L. Ye. *Anal. Chim. Acta* 2007, **584**, 112–121.
33. L. Ye, K. Yoshimatsu, D. Kolodziej, J. C. Francisco and E. S. Dey. *J. App. Pol. Sci*., 2006, **102**, 2863-2867.
34. P. Tonglairoum, W. Chaijaroenluk, T. Rojanarata, T. Ngawhirunpat, P. Akkaramongkolporn and P. Opanasopit. *AAPS PharmSciTech* 2013, **14**, 838–846.
35. D. Bratkowska, N. Fontanals, P. A. G. Cormack, F. Borrull and R. M. Marcé. *J. Chrom. A* 2012, **1225**, 1–7.
36. A. H. Kamel and H. R. Galal, *Int. J. Electrochem. Sci.*, 2014, **9**, 4361 – 4373
37. X. Dong, H. Sun, X. Lü, H. Wang, S. Liu and N. Wang, *Analyst*, 2002, **127**, 1427–1432
38. Z. Sun, W. Schussler, M. Sengl, R. Niessner and D. Knopp, *Anal. Chim. Acta.,* 2008, **620**, 73–81.
39. S. Mallakpour and M. Dinari, *Iranian Pol. J.*, 2011, **20**, 260-279.
40. K. Hong, H. Zhang, J. W. Mays, A. E. Visser, C. S. Brazel, J. D. Holbrey, W. M. Reichert and R. D. Rogers, *Chem. Commun*. 2002, 1368-1369.
41. B. –K. Chen, T. –Y. Wu, Y. –M. Chang and A. F. Chen, *Chem. Eng. J.*, 2013, **215**–**216**, 886–893.
42. Y. Liu, K. Hoshina and J. Haginaka, *Talanta* 2010, **80**, 1712.
43. W. Yao, Y. Fang, G. Li, Z. Gao and Y. Cheng, *Polym. Adv. Tech.,* 2008, **19**, 812.
44. I. A. Nicholls, *Chem. Lett.,* 1995, **24**, 1035.
45. N. W. Turner, N. P. Holmes, C. Brisbane, A. B. McGeachie, C. I. Holdsworth, M. C. Bowyer and A McCluskey, *Soft Matter* 2009, **5**, 3663.
46. X. Sun, J. He, G. R. Cai, A. Q. Lin, W. J. Zheng, X. Liu, L. X. Chen, X. W. He and Y. K. Zhang, *J. Sep. Sci.,* 2010, **33**, 3786–3793.
47. He, J.-X.; Fang, G.-Z.; Yao, Y.-C.; Wang, S. *J. Sep. Sci.* 2010, **33**, 3263–3271.
48. J. N. Sun, Y. F. Hu, W E. Frieze and D. W. Gidley, *Rad. Phys. Chem.*, 2003, **68**, 345-349.
49. A. M. Rosengren, B. C. G. Karlsson and I. A. Nicholls**,** *Int. J. Mol. Sci.* 2013, **14**, 1207-1217.
50. P. Seddon, A. Cooper, K. Scot and, N. Winterton, *Macromolecules* 2003, **36**, 4549-4556.
51. M. J. Whitcombe and E. N. Vulfson, *Adv. Mater.,* 2001, **13**, 467.
52. O. Castell, C. Allender and D. Barrow, *Biosens. Bioelect*. 2006, **22**, 526.
53. O. Kotrotsiou, S. Chaitidou and C. Kiparissides, *Mater. Sci. Engin. C*. 2009, **29**, 2141.
54. M. Whitcombe and E. Vulfson, *Adv. Mat.* 2001, **13**, 467.
55. C. Philip and B. Matthew, *J. Macromol. Sci. A,* 2008, **45**, 335.
56. D. Cleland and A. McCluskey, *Org. Biomol. Chem.,* 2013, **11**, 4646.
57. D. Cleland and A. McCluskey, *Org. Biomol. Chem.,* 2013, **11**, 4672.
58. D. Cleland, D. D.. Olsson, B. C. G. Karlsson, I. A. Nicholls and A. McCluskey, *Org. Biomol. Chem.*, 2014, **12**, 844.
59. Y. Zhang, D. Song, L. M. Lanni and K. D. Shimizu. *Macromolecules*, 2010, **43**, 6284.
60. Y. Zhang, D. Song, J. C. Brown and K. D. Shimizu. *Org. Biomol. Chem.* 2011, **9**, 120.
61. J. G. Huddleston, A. E. Visser, W. M. Reichert, H. D. Willauer, G. A. Broker and R. D. Rogers, *Green Chem.*, 2001, **3**, 156.
62. A. Triolo, O. Russina, H. –J. Bleif and E. Di Cola, *J. Phys. Chem. B,* 2007, **111**, 4641.
63. M. J. S. Dewar, E. G. Zoebisch, E. F. Healy, J. J. P. Stewart, *J. Am. Chem. Soc.*, 1985, **107**, 3902.
64. Spartan '04, Wavefunction, Inc., Irvine California USA.
65. L. Schwarz, M. C. Bowyer, C. I. Holdsworth and A. McCluskey, *Aus. J. Chem.*, 2006, **59**, 129.
66. C. M. Phillip and B. Mathew, *J. Macromol. Sci., Part A: Pure Appl. Chem.*, 2008, **45**, 335.
67 N. W. Turner, C. I. Holdsworth, S. W. Donne, A. McCluskey and M. C. Bowyer, *New J. Chem.* 2010, **34**, 686.
68. S. Brunauer, P. H. Emmett and E. Teller, *J. Am. Chem. Soc.* 1938, **60**, 309.
69. S. J. Tao, *J. Chem. Phys.*, 1972, **56**, 5499–5510.
70. M. Eldrup, D. Lightbody and J. N. Sherwood, *Chem. Phys.*, 1981, **63**,51–58]
71. T. L. Dull, W. E. Frieze, D. W. Gidley, J. N. Sun and A. F. Yee, *J. Phys. Chem. B*, 2001, 105, 4657–4662.]

[a] *Discipline of Chemistry, University of Newcastle, Callaghan, NSW 2308, Australia. Fax:+61 2 4921 5472; Tel: +61 2 4921 5472; E-mail: Adam.McCluskey@Newcastle.edu.au*
[b] *CSIRO, Materials Science and Engineering, Private Bag 33, Clayton South MD`C. Victoria 3169, Australia*
[c] *Discipline of Applied Sciences, School of Environmental & Life Sciences, University of Newcastle, Ourimbah, NSW 2258, Australia.*

† Electronic Supplementary Information (ESI) available: [details of any supplementary information available should be included here]. See DOI: 10.1039/b000000x/

‡ The NIP is the non-imprinted polymer synthesised in exactly the same manner as the MIP except for the addition of the template.